TECHNICAL REPORT ARLCB-TR-80029

STRAIN BEHAVIOR OF PRESSURIZED CRACKED THICK-WALLED CYLINDERS

J. F. Throop
R. R. Fujczak

August 1980

US ARMY ARMAMENT RESEARCH AND DEVELOPMENT COMMAND
LARGE CALIBER WEAPON SYSTEMS LABORATORY
BENÉT WEAPONS LABORATORY
WATERVLIET, N. Y. 12189

AMCMS No. 612105H840011

DA Project No. 1L162105AH84

PRON No. 1A0217131A1A

DISCLAIMER

The findings in this report are not to be construed as an official Department of the Army position unless so designated by other authorized documents.

The use of trade name(s) and/or manufacturer(s) does not constitute an official indorsement or approval.

DISPOSITION

Destroy this report when it is no longer needed. Do not return it to the originator.

SECURITY CLASSIFICATION OF THIS PAGE (When Data Entered)

REPORT DOCUMENTATION PAGE		READ INSTRUCTIONS BEFORE COMPLETING FORM
1. REPORT NUMBER ARLCB-TR-80029	2. GOVT ACCESSION NO.	3. RECIPIENT'S CATALOG NUMBER
4. TITLE (and Subtitle) STRAIN BEHAVIOR OF PRESSURIZED CRACKED THICK-WALLED CYLINDERS		5. TYPE OF REPORT & PERIOD COVERED 6. PERFORMING ORG. REPORT NUMBER
7. AUTHOR(s) J. F. Throop and R. R. Fujczak		8. CONTRACT OR GRANT NUMBER(s)
9. PERFORMING ORGANIZATION NAME AND ADDRESS Benet Weapons Laboratory Watervliet Arsenal, Watervliet, NY 12189 DRDAR-LCB-TL		10. PROGRAM ELEMENT, PROJECT, TASK AREA & WORK UNIT NUMBERS AMCMS No. 612105H840011 DA Project No. 1L162105AH84 PRON No. 1A0217131A1A
11. CONTROLLING OFFICE NAME AND ADDRESS US Army Armament Research and Development Command Large Caliber Weapon Systems Laboratory Dover, NJ 07801		12. REPORT DATE August 1980 13. NUMBER OF PAGES 26
14. MONITORING AGENCY NAME & ADDRESS(if different from Controlling Office)		15. SECURITY CLASS. (of this report) Unclassified 15a. DECLASSIFICATION/DOWNGRADING SCHEDULE

16. DISTRIBUTION STATEMENT (of this Report)

Approved for public release; distribution unlimited.

17. DISTRIBUTION STATEMENT (of the abstract entered in Block 20, if different from Report)

18. SUPPLEMENTARY NOTES

To be published in Experimental Mechanics.

19. KEY WORDS (Continue on reverse side if necessary and identify by block number)

Fatigue Cracks
Crack Shape
Thick Wall Cylinders
Strain Measurements
Autofrettage
Lame Strain
Ultrasonics

20. ABSTRACT (Continue on reverse side if necessary and identify by block number)

External circumferential strains were measured on large thick wall pressure vessels containing internal fatigue cracks, using bonded strain gages. When strains measured over the cracks become compressive they predict impending failure. Normalization by the Lame strain relates them to the fraction of fatigue life consumed and provides estimates of longevity.

DD FORM 1 JAN 73 1473 EDITION OF 1 NOV 65 IS OBSOLETE

UNCLASSIFIED

SECURITY CLASSIFICATION OF THIS PAGE (When Data Entered)

TABLE OF CONTENTS

LIST OF FIGURES

ACKNOWLEDGMENTS

We express our appreciation to R. R. Lasselle who conceived the strain monitoring technique, R. T. Abbott for instrumentation and testing, C. A. Monarch for drafting, and C. J. Crell for illustrations. We also dedicate this work to the memory of Mike Lombard whose enthusiasm gave us a good start but who didn't make it all the way.

LIST OF SYMBOLS

a	=	crack depth
$a/2c$	=	aspect ratio, crack depth to length
$a/(R_2-R_1)$	=	ratio of crack depth to wall thickness
D_i	=	inside diameter
D_o	=	outside diameter
L	=	cylinder specimen length
N	=	fatigue cycles
N_f	=	cycles for failure
P	=	internal hydraulic pressure
R	=	radius to any point inside cylinder wall
R_a	=	radius from center to crack tip
R_1	=	inside radius
R_2	=	outside radius
t	=	wall thickness
x	=	ratio of cycles at a given crack depth to the cycles for failure
y	=	ratio of measured strain in the crack plane to the theoretical Lamé strain on the outside of an uncracked cylinder
$2c$	=	longitudinal length of crack
% OS	=	percent overstrain
ε	=	measured circumferential strain
ε_o	=	measured circumferential strain at crack plane
ε_{th}	=	theoretical Lamé strain at OD of uncracked cylinder

$\varepsilon_o/\varepsilon_{th}$ = ratio of crack plane strain to Lamé strain

ϕ = angle from crack plane

σ = stress

σ_I = internal stress at crack tip

σ_o = stress on outside surface

σ_y = yield stress

σ/P = ratio of stress to pressure

INTRODUCTION

An experimental method for measuring crack growth of internally cracked thick-walled cylinders under pressure was developed by Lasselle.[1] The strain pattern on the outside surface of the cylinder deviates from the Lame´ strain behavior as the crack grows outward through the cylinder wall. Shannon[2] has pointed out from the experimental data of Lasselle that the pressure-bending effect on the outside of the cylinder is mainly confined to the surface region between ± 7 degrees of the plane of the radial crack. He concluded that strain measurements will measure crack depth accurately and will detect changes in crack depth with the same sensitivity as a crack-opening-displacement gage when used with high-strength materials. The major advantage of the local-strain-sensing technique is the relative ease with which it can be used for automated monitoring of crack growth.

In order to enhance our understanding of the crack growth behavior of internally pressurized cylinders, we have studied the relationship of the external experimental circumferential strains of the cylinders as functions of pressure, increasing crack depth, crack shape and percent overstrain. The stresses and strains are compared with theoretical Lame´ values for the uncracked specimen. This study is a continuation of the study of cracked

[1] Underwood, J. H., Lasselle, R. R., Scanlon, R. D., and Hussain, M. A., "A Compliance K-Calibration for a Pressurized Thick-Walled Cylinder With a Radial Crack," Eng. Fract. Mech., 4, 231-44, (1972).

[2] Shannon, R. W. E., "Crack Growth Monitoring by Strain Sensing," Pres. Ves. & Piping, (1), pp. 61-73, Appl. Science Publ. Ltd, England (1973).

C-shaped specimens[3] reported previously. The results show that suitable choice of gage location and appropriate calibration relationships can enable automatic strain-gage monitoring of crack growth and prediction of failure in thick-walled cylinders.

APPARATUS, INSTRUMENTATION, AND PROCEDURE

The strains on the external surface of 30 inch (0.76 m) long cylinders of high strength steel were measured with bonded foil strain gages while pressurized in steps from zero to 48 ksi (330 MPa). The cylinders were 7.1 inches (180 mm) bore diameter with 14.25 inches (360 mm) outside diameter and were fatigue cracked from longitudinal internal notches. Three initial notch geometries were used; semicircular, 4 inch (100 mm) and 20 inch (500 mm) long notches produced by electrical discharge machining. They were 1/4 inch (6.4 mm) deep by 0.030 inch (0.76 mm) wide, the semicircular notch being 1/2 inch (13 mm) diameter half-penny shape. The external strains on the periphery at mid-section of the cylinder were measured at crack depths 1/4 inch (6.4 mm) to 3 inches (76 mm) measured from the bore, generally at intervals of 1/2 inch (13 mm).

Figure 1 shows a schematic diagram of a typical cylinder with initial notch and the growth of a 20 inch (500 mm) long notch from 1/4 inches (6.4 mm) initial depth by repeated pressurization to 48 ksi (330 MPa).

[3] Throop, J. F. and Fujczak, R. R., "Stress, Strain and Deflection of Cracked C-Shaped Specimens," Experimental Mechanics, Vol. 17, No. 8, pp. 290-296, (1977).

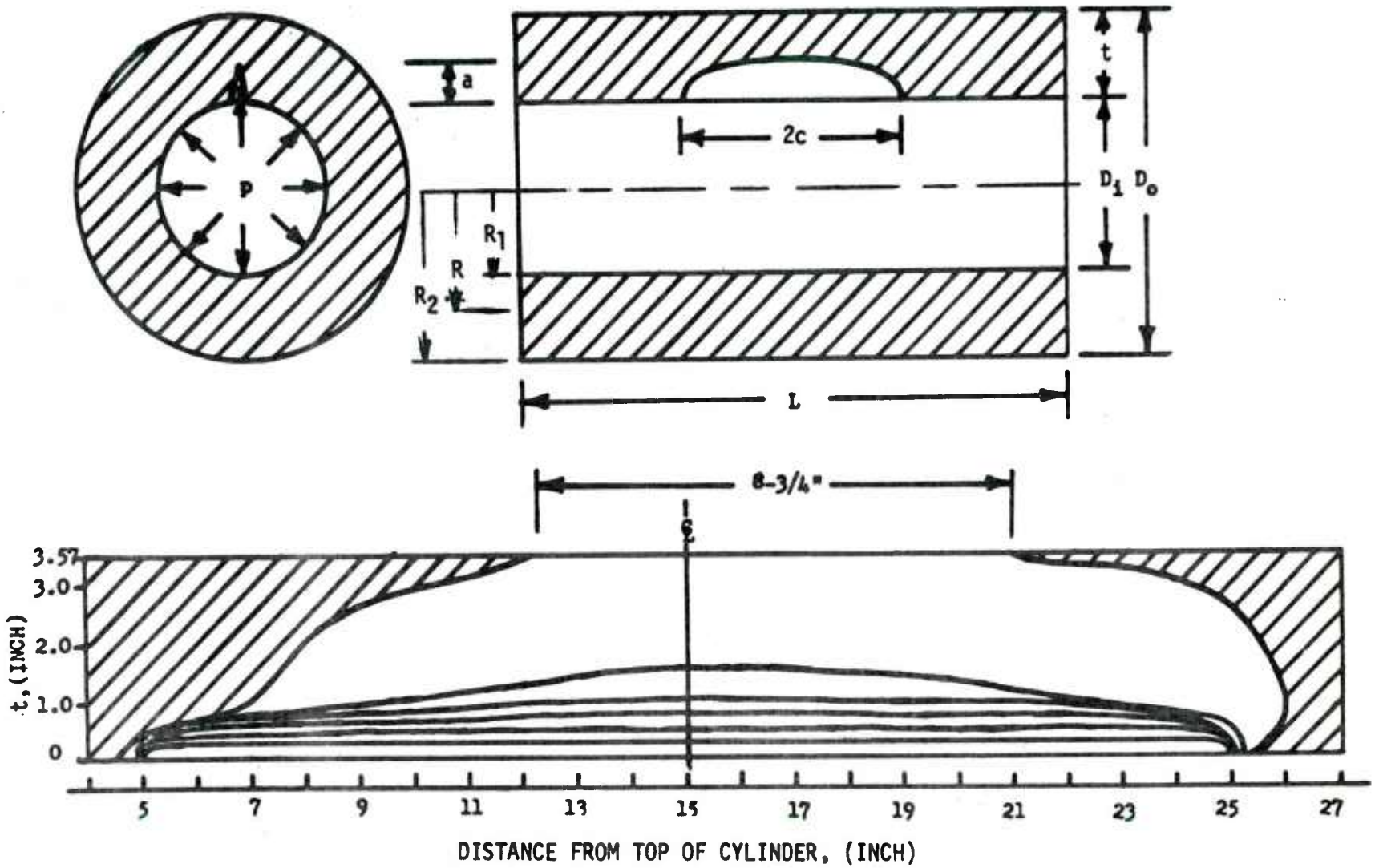

Fig. 1 PRESSURIZED CRACKED CYLINDER

The gages were mounted circumferentially with two directly over the notch line, equally spaced on either side of the cylinder midsection, and at 5°, 15°, 30°, 60°, 90°, 135°, and 180° on either side of the notch. Strain measurements were made on non-autofrettaged cylinders, and on cylinders with 30% overstrain and 60% overstrain produced by hydraulic autofrettage. The percent overstrain is the portion of the wall thickness which has exceeded the material yield strength during the prestressing by overpressurization. Specimens with single notch, two opposing notches and four equally spaced notches were tested. The bore of the cylinder was partially filled with a cylindrical steel mandrel which supported the end closures, leaving the cylinder in essentially the open-end condition. A synthetic hydraulic oil was used as the pressurizing medium, filling the remainder of the cavity including the notch. Fatigue cracks grown from the initial notches were monitored for depth and shape with ultrasonics periodically as the cylinder was repeatedly pressurized from 4 ksi (28 MPa) to 48 ksi (330 MPa). The growth of fatigue cracks in cylinder specimens is described by Throop[4] and the 175 mm fatigue specimens, end packing, and ultrasonic crack depth measurements are described by Davidson et al.[5]

[4]Throop, J. F., "Fatigue Crack Growth in Thick-Walled Cylinders," Proceedings National Conference on Fluid Power, Vol. XXVI, pp. 115-131, NCFP, Chicago, (1972).

[5]Davidson, T. E., Throop, J. F., and Reiner, A. N., "The Role of Fracture Toughness and Residual Stresses in the Fatigue and Fracture Behavior of Large Thick-Walled Pressure Vessels," Proceedings National Conference on Fluid Power, Vol. XXVI, pp. 102-114, NCFP, Chicago, (1972).

The strain readings were taken under static pressurization using a null-balancing technique, and up to 20 gages were recorded at several pressures to maximum pressure and back to zero again.

STRESS AND STRAIN EQUATIONS

(a) The stress and strain on the outside surface and stress on the inside surface may be calculated by the following equations:[6]

$$\sigma_o = P \frac{2R_1^2}{(R_2^2 - R_1^2)} \qquad \text{on outside surface} \qquad (1)$$

$$\varepsilon_{th} = \frac{P}{E} \frac{2R_1^2}{(R_2^2 - R_1^2)} \qquad \text{on outside surface} \qquad (2)$$

$$\sigma_I = P \frac{(R_2^2 + R_1^2)}{(R_2^2 - R_1^2)} \qquad \text{on inside surface} \qquad (3)$$

(b) Cylinder radial displacement may be related to circumferential surface strain by the following equation:

Circumferential surface strain equals cylinder unit radial displacement:

$$\varepsilon_{circ} = \frac{2\pi(R + \Delta R) - 2\pi R}{2\pi R} = \frac{\Delta R}{R} \qquad (4)$$

So the radial deformation, ΔR, may be calculated by the following equation:

$$\Delta R = R \times \varepsilon_{circ} \qquad (5)$$

---

[6] Timoshenko. S. P. and Goodier, J. N., Theory of Elasticity, Third Edition, McGraw-Hill Book Company, New York, pp. 68-71 (1970).

(c) An idealization presented by Shannon[2] assumes wall thinning represented by an effective increase of the internal radius of the cylinder to include the crack depth, with the pressure-bending effect applied as a moment on a section of depth equal to the remaining wall thickness of the cylinder. Thus, the equations for stress and strain on the outside surface are as follows.

Uniform-thinning and pressure-bending approximation for stress and strain in cylinder with internal longitudinal straight-fronted crack of depth $a = (R_a - R_1)$; (Shannon, 1973):

Outside Surface:

$$\sigma_o = \frac{2PR_a^2}{(R_2^2 - R_a^2)} - \frac{3P(R_a - R_1)(R_2 - R_1)}{(R_2 - R_a)^2} \tag{6}$$

$$\varepsilon_o = \frac{\sigma_o}{E} \tag{7}$$

A similar expression approximating the stress at the inside of the crack is:

$$\sigma_I = P\frac{(R_2^2 + R_a^2)}{(R_2^2 - R_a^2)} + \frac{3P(R_a - R_1)(R_2 - R_1)}{(R_2 - R_a)^2} \tag{8}$$

These equations are plotted in Figure 9 which will be discussed later.

EXPERIMENTAL RESULTS

The approximately 200 strain readings at each crack depth were computer-smoothed with an interpolating spline function to provide a continuous expression of strains around the periphery at the cylinder midsection. The

[2]Shannon, R. W. E., "Crack Growth Monitoring by Strain Sensing," Pres. Ves. & Piping, (1), pp. 61-73, Appl. Science Publ. Ltd., England (1973).

results were plotted in two forms: (a) strain versus equatorial angle in rectangular coordinates, and (b) circumferential strain plotted as a radial vector in polar coordinates. The latter plot forms an interesting figure which, in the case of a single crack, is heart-shaped with the cusp directly over the crack plane, like a cardioid. This plot is shown in Figure 2. Note that the cusp coincides with the crack plane. For zero crack depth, a = 0, the Lame´ theoretical strain plots as a circle.

In the case of multiple cracks, as shown in Figure 3, the shape becomes like an epicycloid, where for dual opposing notches (Figure 3a) the two cusps occur directly over the cracks, and for four notches (Figure 3b), there are four cusps directly over the four cracks.

These figures are significant since it is shown by Equations (4) and (5) that the external circumferential strain at a point on a cylinder is equal to the actual unit radial deformation $\Delta R/R$ at that same point. Hence the radial deformation is proportional to the circumferential strain and the shape of the figure is an exaggerated representation of the distorted shape of the cracked pressurized cylinder. When compared with the theoretical Lame´ circumferential strain for the given pressure, the figure shows the difference in shape of the cracked cylinder from that of an uncracked cylinder at pressure. The consequent bending of the cylinder wall at the sites of sharp curvature and the sites of cusps in the figure therefore becomes apparent, although exaggerated.

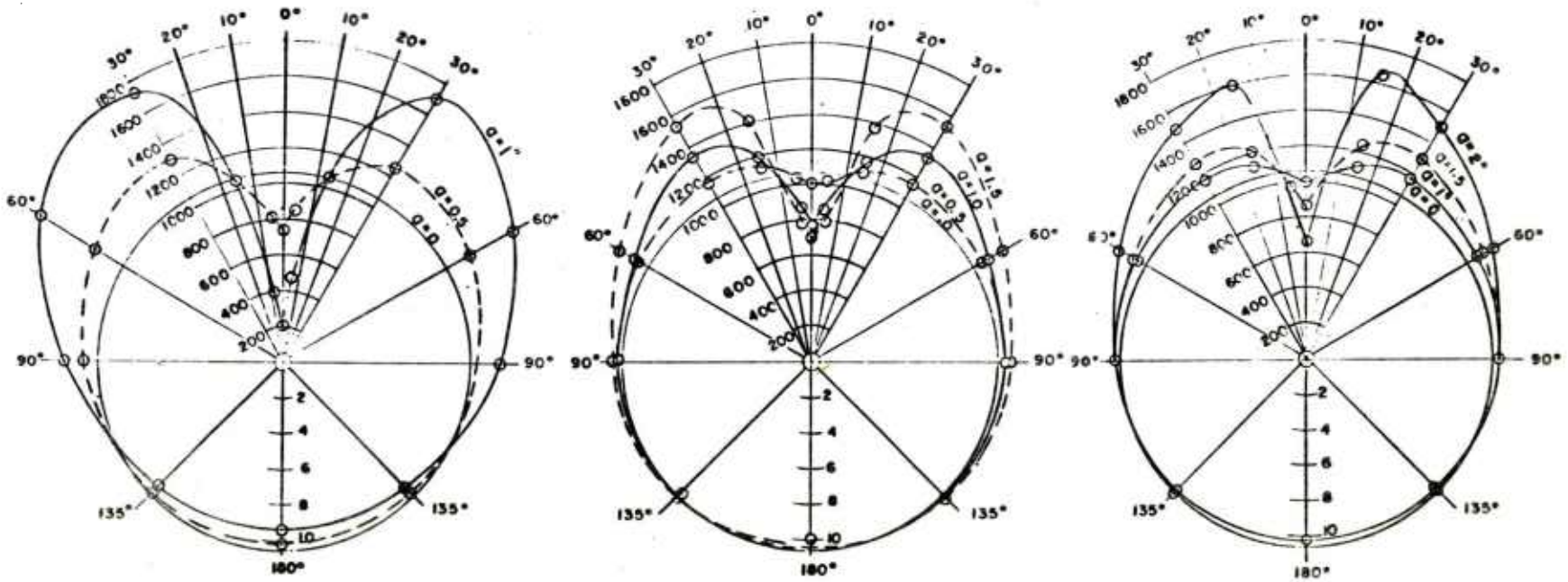

Fig. 2 POLAR PLOT OF STRAINS IS SIMILAR TO A CARDIOID.

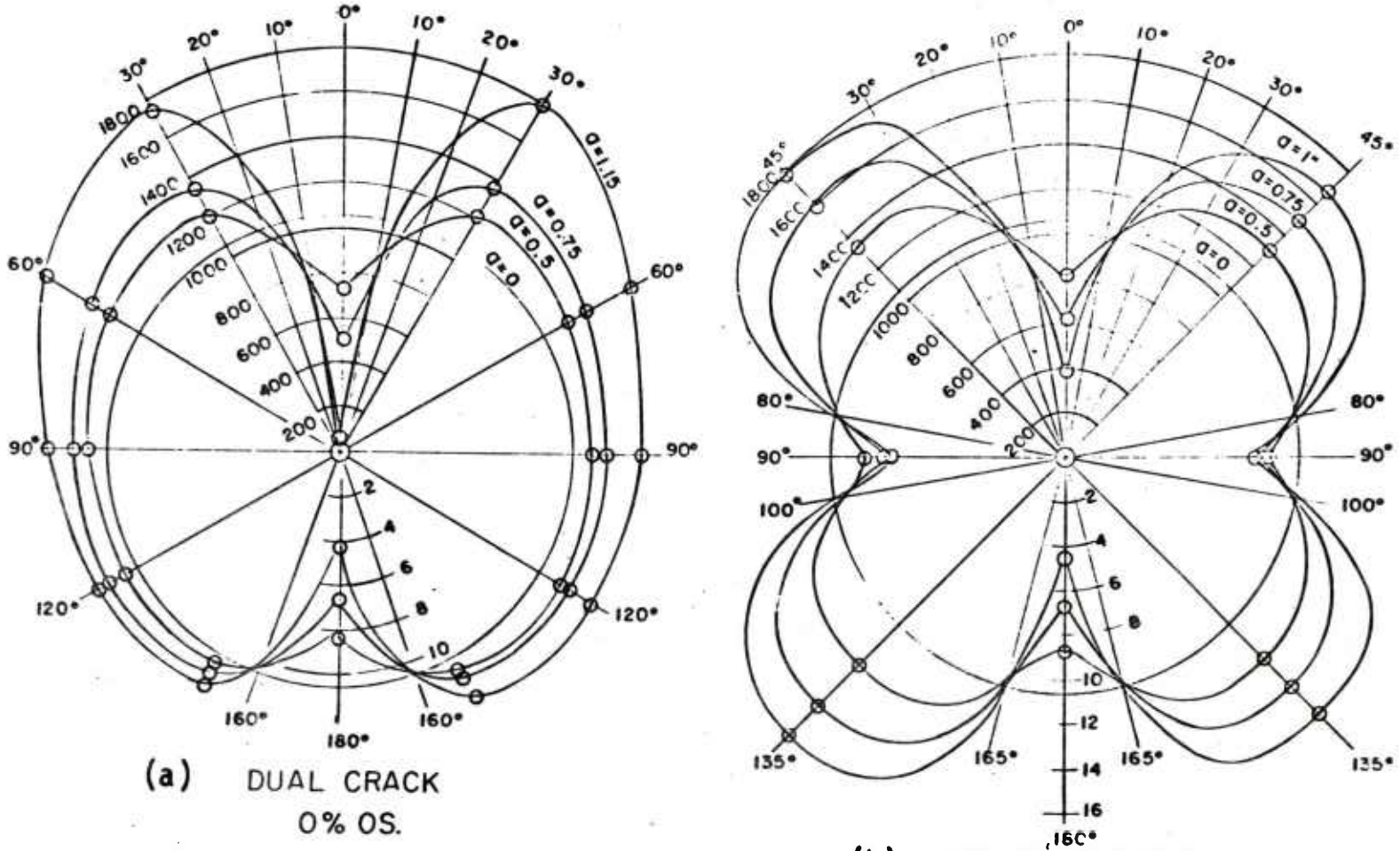

(a) DUAL CRACK
0% OS.

(b) FOUR CRACKS
0% OS.

Fig. 3 POLAR PLOT FOR MULTIPLE CRACKS IS SIMILAR TO AN EPICYCLOID.

It is found that the greatest decrease from the Lame´ strain occurs directly over the crack, while the greatest increase above the Lame´ strain occurs at approximately 15° on either side of the crack. At angles remote from the crack the strains remain approximately equal to the Lame´ strain for the given pressure.

It is also found that as the crack deepens, the strain directly over the crack diminishes from the tensile Lame´ strain expected in an uncracked cylinder and approaches zero strain in a regular manner with increasing crack depth. When this strain reaches zero or becomes compressive the fracture of the cylinder is imminent. During this time the pressure within the crack is exerting a bending moment on the remaining ligament as well as adding to the circumferential tension, and the compressive strain on the outside of the ligament becomes greater than the circumferential tensile strain. When the remaining ligament finally becomes thin enough the tension in it once again exceeds the bending strains and stretches the ligament to failure. In tough and ductile steel this may simply result in a small leak in the cylinder wall as the crack pierces it. Even this type of failure releases a large amount of strain energy, whereas a brittle fracture would result in fragmentation. In either case the decrease of tensile strain over the crack provides a warning preceding failure.

Figures 4 and 5 show that autofrettage by overstrain of the cylinders increases the crack tolerances. Figure 4, the polar plot for 30% overstrained cylinders, shows a greater crack tolerance than Figure 2, since at the cusp the decrease from the Lame´ theoretical strain is less, for instance, at crack

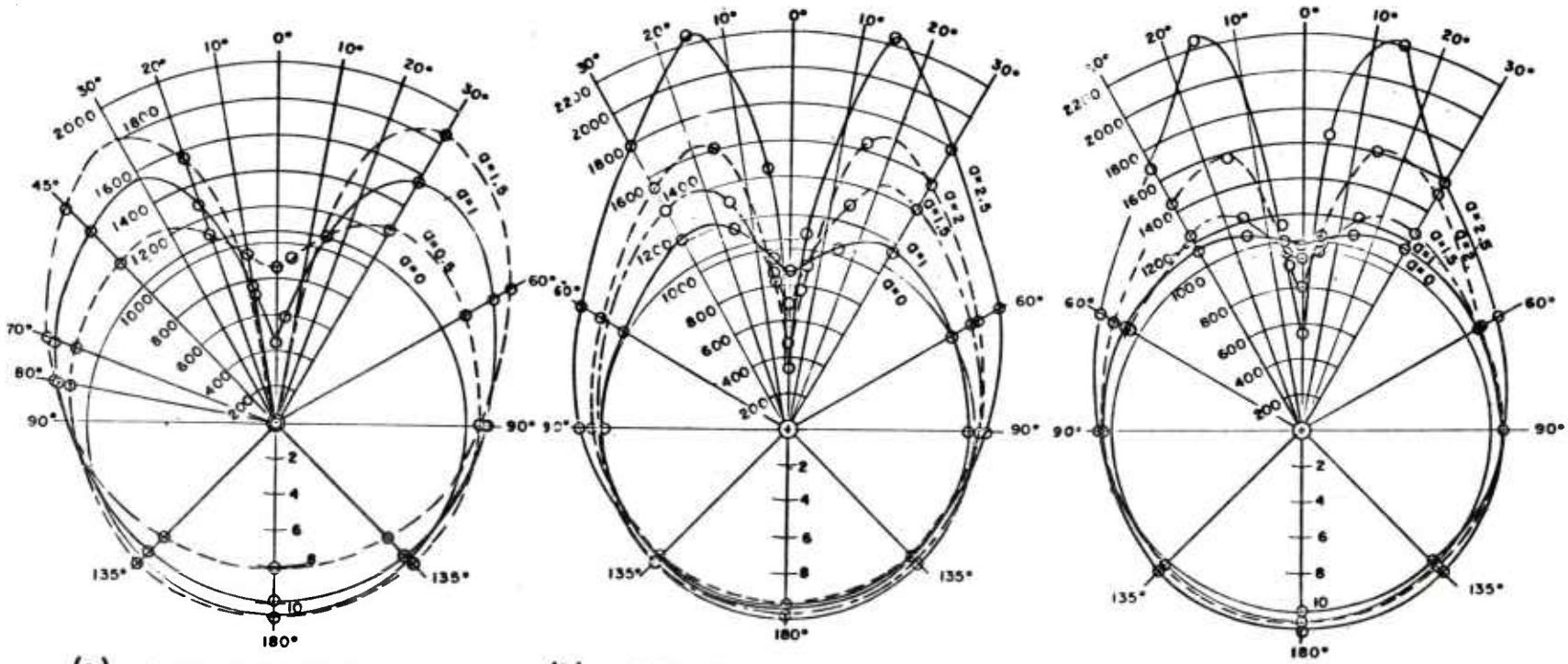

Fig. 4 POLAR PLOT FOR 30% OVERSTRAINED CYLINDERS SHOWS INCREASED CRACK TOLERANCE.

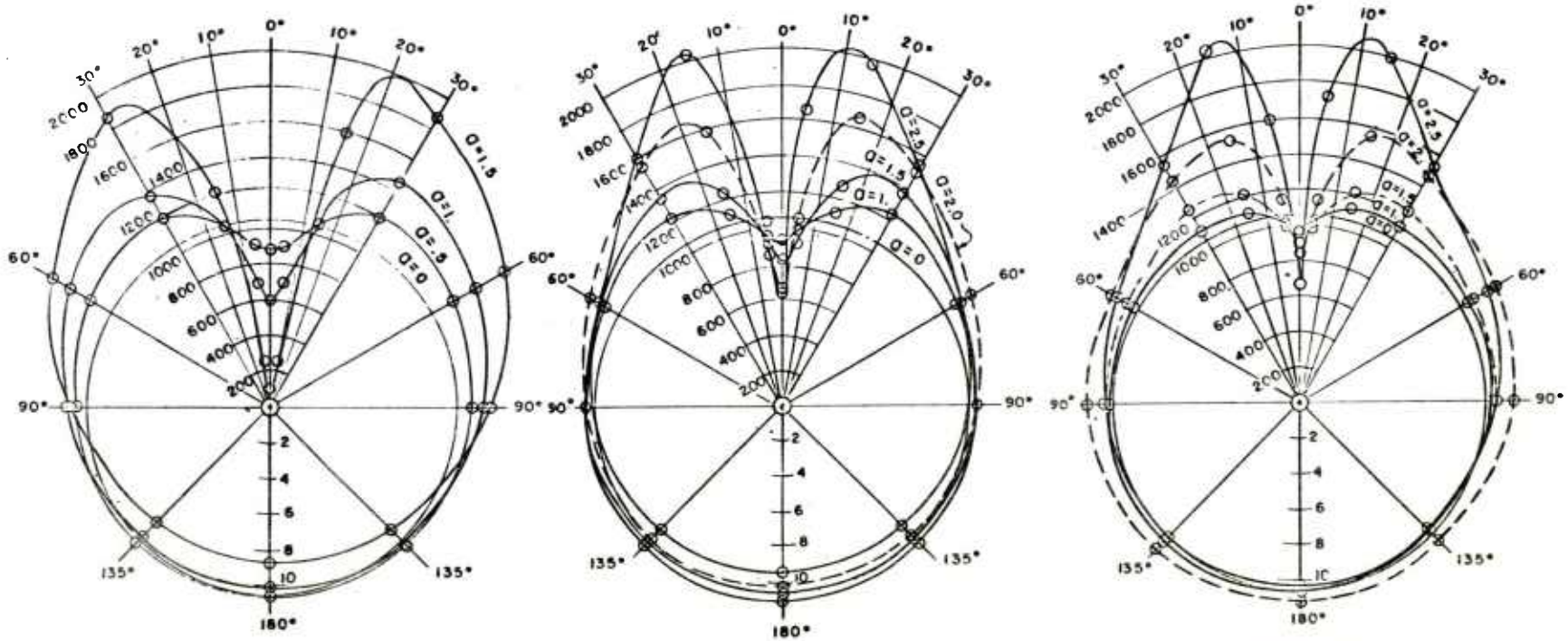

Fig. 5 POLAR PLOT FOR 60% OVERSTRAINED CYLINDERS SHOWS STILL GREATER CRACK TOLERANCE.

depth a = 1 inch, than that of the corresponding non-autofrettaged cylinder. Figure 5, the polar plot for 60% overstrained cylinders, shows still greater crack tolerance. The cusps are shallower and the peak strains are closer to the crack plane, indicating increased resistance to the crack opening.

Figure 6 shows crack depth plotted versus number of fatigue loadings for 0%, 30%, and 60% overstrained cylinders with long curved cracks, semi-elliptical cracks and semicircular cracks. It is noted that the fatigue life increases with percent overstrain and also with aspect ratio a/2c of the crack, going from a/2c = .012 for the long curved crack to a/2c = .250 for the semi-elliptical crack and to a/2c = .500 for the semicircular crack.

Figure 7 indicates strain measured at the crack plane, $\phi = 0°$, plotted versus number of fatigue loadings for 0%, 30%, and 60% overstrained cylinders with long curved cracks, semi-elliptical cracks, and semicircular cracks. In all cases the strain diminishes to zero and becomes compressive (negative) as failure is approached, and suddenly goes tensile at failure. This terminal phenomenon indicates that the bending effect measured by the external strains is overcome by the tensile effect as the remaining ligament becomes smaller and cannot support the bending moment any longer.

Figure 8 shows the strain ratio, $\varepsilon_o/\varepsilon_{th}$, of the crack-plane strain to the theoretical strain plotted versus "a", the crack depth. The dashed curves are calculated from Shannon's uniform wall thinning and pressure bending idealization for a straight-fronted crack in a non-autofrettaged cylinder, the crack depth for any strain for a curved front being a multiple of that for the straight front. Curves for 0%, 30%, and 60% overstrained cylinders are

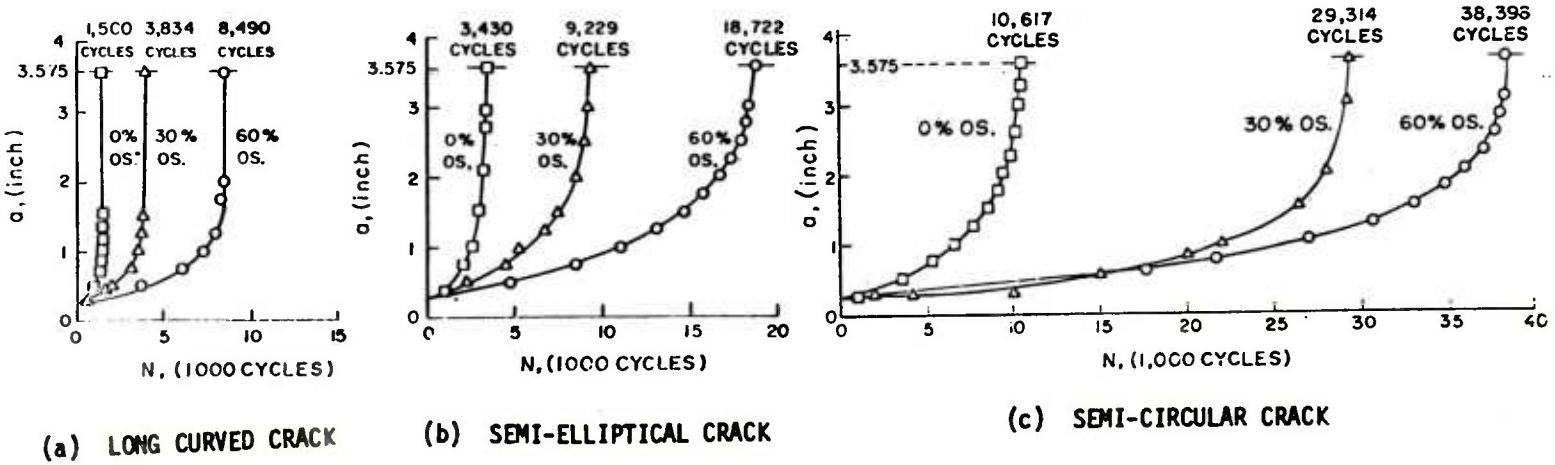

(a) LONG CURVED CRACK (b) SEMI-ELLIPTICAL CRACK (c) SEMI-CIRCULAR CRACK

Fig. 6 CRACK DEPTH PLOTTED VERSUS NUMBER OF FATIGUE LOADINGS.

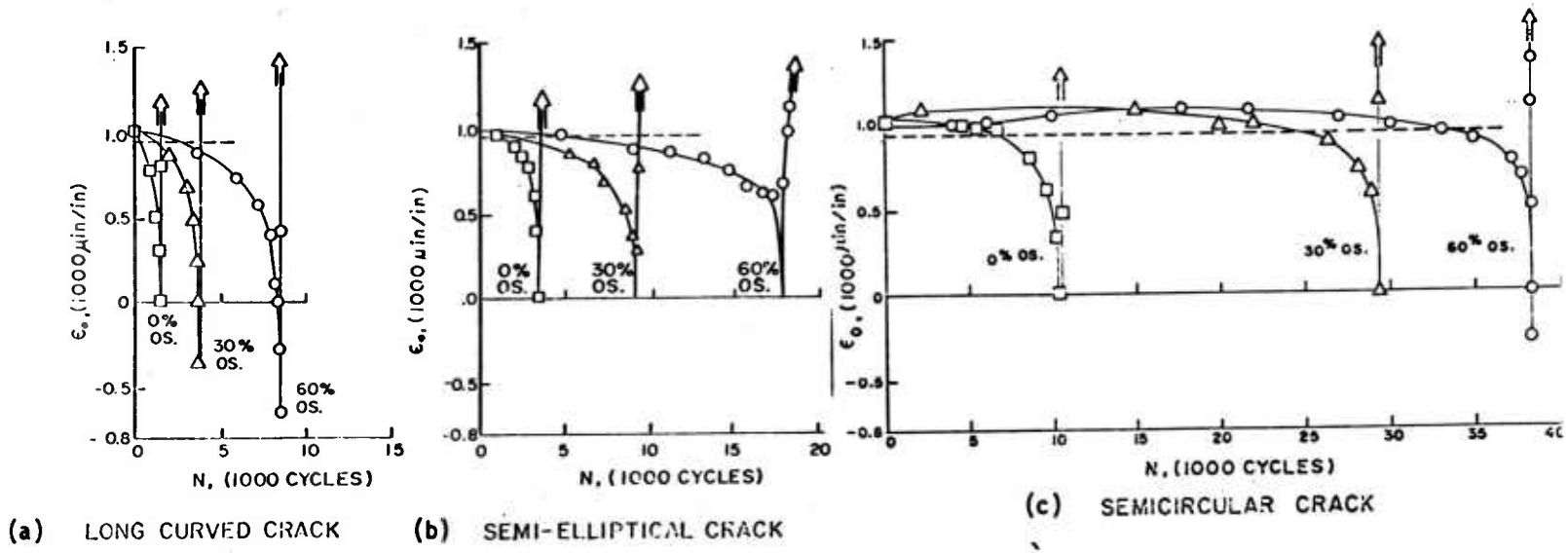

Fig. 7 STRAIN MEASURED AT CRACK PLANE, $\phi = 0$, PLOTTED VERSUS NUMBER OF FATIGUE LOADINGS.

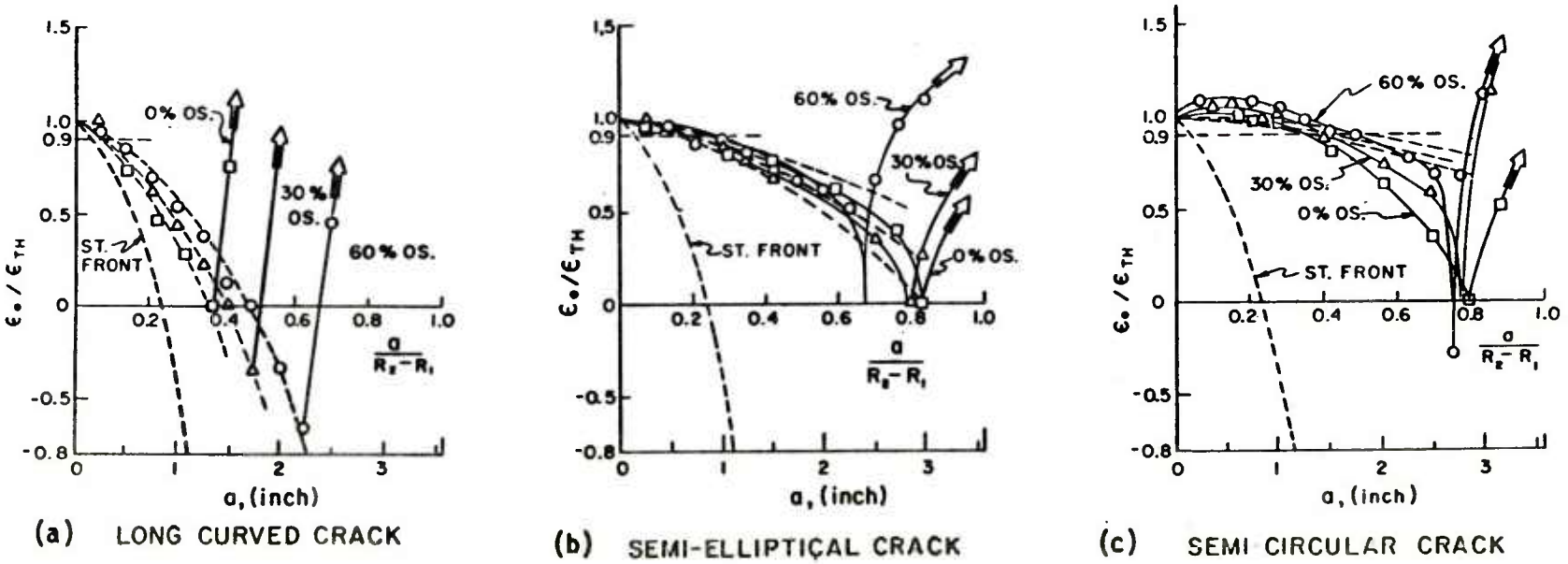

Fig. 8 STRAIN RATIO, ϵ_o/ϵ_{th}, OF THE ZERO-ANGLE STRAIN TO THE THEORETICAL STRAIN PLOTTED VERSUS CRACK DEPTH.

compared for long curved cracks, semi-elliptical cracks and semicircular cracks. The data is approximated by these calculated curves until a 10% reduction of $\varepsilon_o/\varepsilon_{th}$ is exceeded, after which the measured values decrease more rapidly than the calculated curves as failure is approached.

Figure 9 shows σ_o/P for external stress calculated from Equation (6) and plotted versus crack depth. This graph shows that Equation (6) represents a decreasing stress, and hence Equation (7) represents a decreasing strain, at the OD as the crack depth is increased for a given value of pressure P. At some crack depth, therefore, the OD strain over the crack will have decreased from the theoretical Lame´ tensile value for that pressure (Eq. (1)), passed through zero and become compressive (negative), as shown at $a/(R_2-R_1)$ equal to about 0.25 in Figure 9. As indicated in Figure 8, failure of the test specimens occurred soon after the strain became compressive (negative), but at a greater crack depth than calculated for the straight-fronted crack.

Figure 9 also shows σ_I/P for internal stress at the crack tip calculated from Equation (8). This shows that Equation (8) starts at a stress given by Equation (3) for zero crack depth and increases with increasing crack depth for a given value of pressure P. In Figure 9 it gives a stress that becomes equal to the yield strength of 170 ksi (1172 MPa) for this particular material at approximately the depth where the OD strain becomes compressive in these specimens. Continued cyclic yielding at the crack tip leads to rapid fatigue failure from this crack depth because the remaining ligament can no longer support bending and behaves more like a thin wall cylinder in the crack zone as the remaining ligament gets thinner.

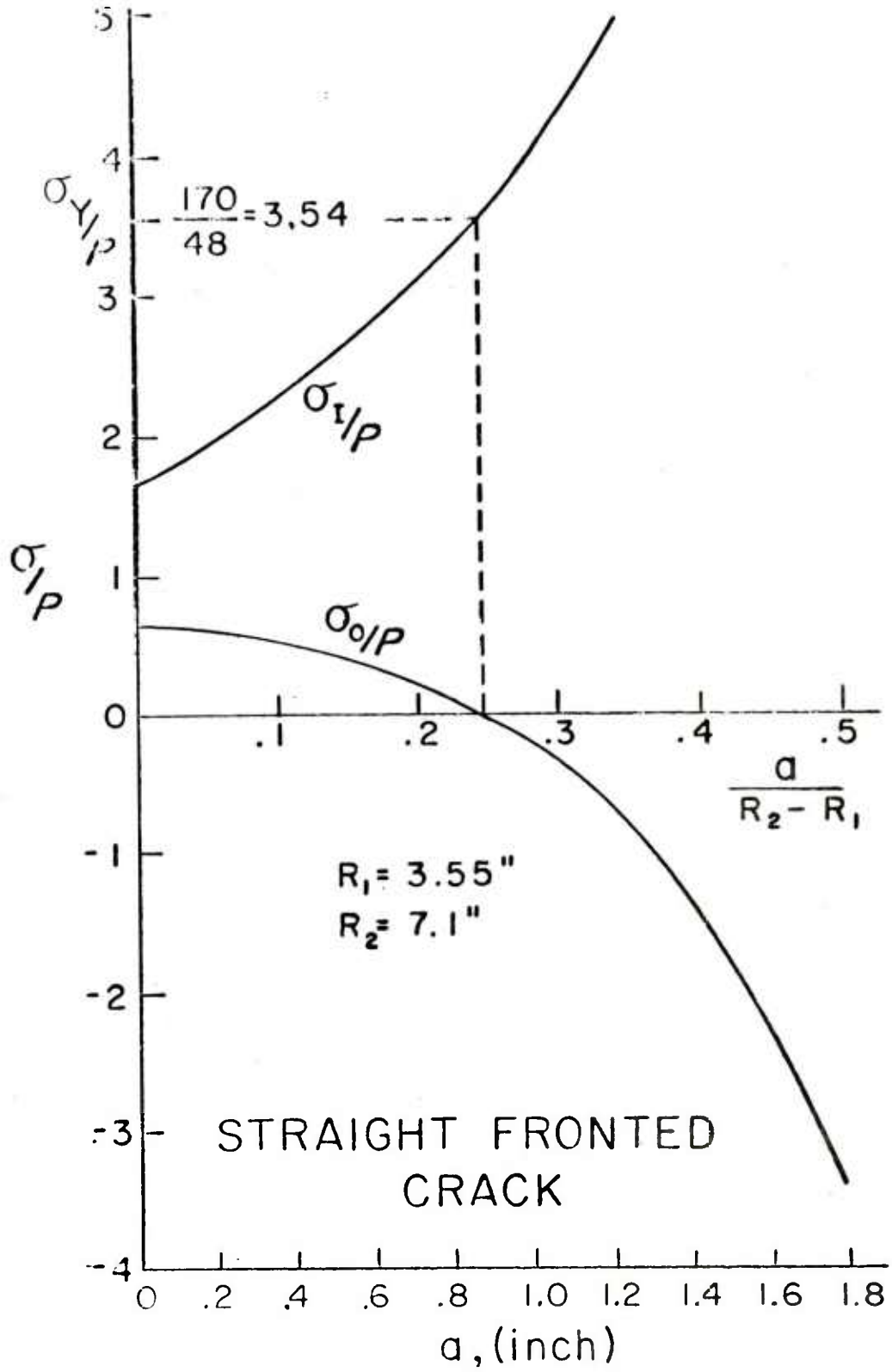

Fig. 9 PLOT OF CALCULATED σ_O/P FOR EXTERNAL STRESS AND σ_I/P FOR INTERNAL STRESS AT THE CRACK TIP.

Figure 10 shows a plot of strain ratio, $\varepsilon_o/\varepsilon_{th}$, versus fraction of fatigue life. The form of curve indicates that fraction of fatigue life is a function of the initial notch shape and relatively insensitive to the percent overstrain, even though percent overstrain enhances absolute fatigue life. The results for the long curved cracks (20 inch notch) fall in a band with the lower bound expressed by the ellipse. Those for the semi-elliptical cracks (4 inch notch) fall in a higher band and those for the semicircular cracks (1/2 inch notch) fall in the highest band. As indicated, the results for 0%, 30%, and 60% overstrained cylinders fall in the band for the given crack shape, indicating that the fraction of life expended is relatively insensitive to the percent overstrain. However, the higher the aspect ratio, a/2c, the greater the fraction of life, N/N_f, that will have been expended when ε_o has decreased to 90% of ε_{th}, as may be seen in Figure 10.

As an example of the possible use of Figure 10, consider a similar sized cylinder which has been subjected to 10,000 pressure cycles, and upon inspection is found to have a radial crack at the bore. If ultrasonic measurements show that the crack is 0.5 inch deep and 2 inches long, the aspect ratio is $a/2c = 0.25$, which corresponds to the middle band on Figure 10. If a circumferential strain gage mounted on the outside surface over the crack reads a strain that is 70% of the theoretical strain for the uncracked cylinder at the same pressure, the fraction of life N/N_f for $\varepsilon_o/\varepsilon_{th} = 0.7$ can be read from Figure 10. This gives a maximum $N/N_f = 0.9$, or $N_f = 11{,}100$ cycles, and a minimum $N/N_f = 0.8$, or $N_f = 12{,}500$ cycles. Thus failure is imminent and should be expected within the next 1,100 to 2,500 cycles if the pressure cycling is continued.

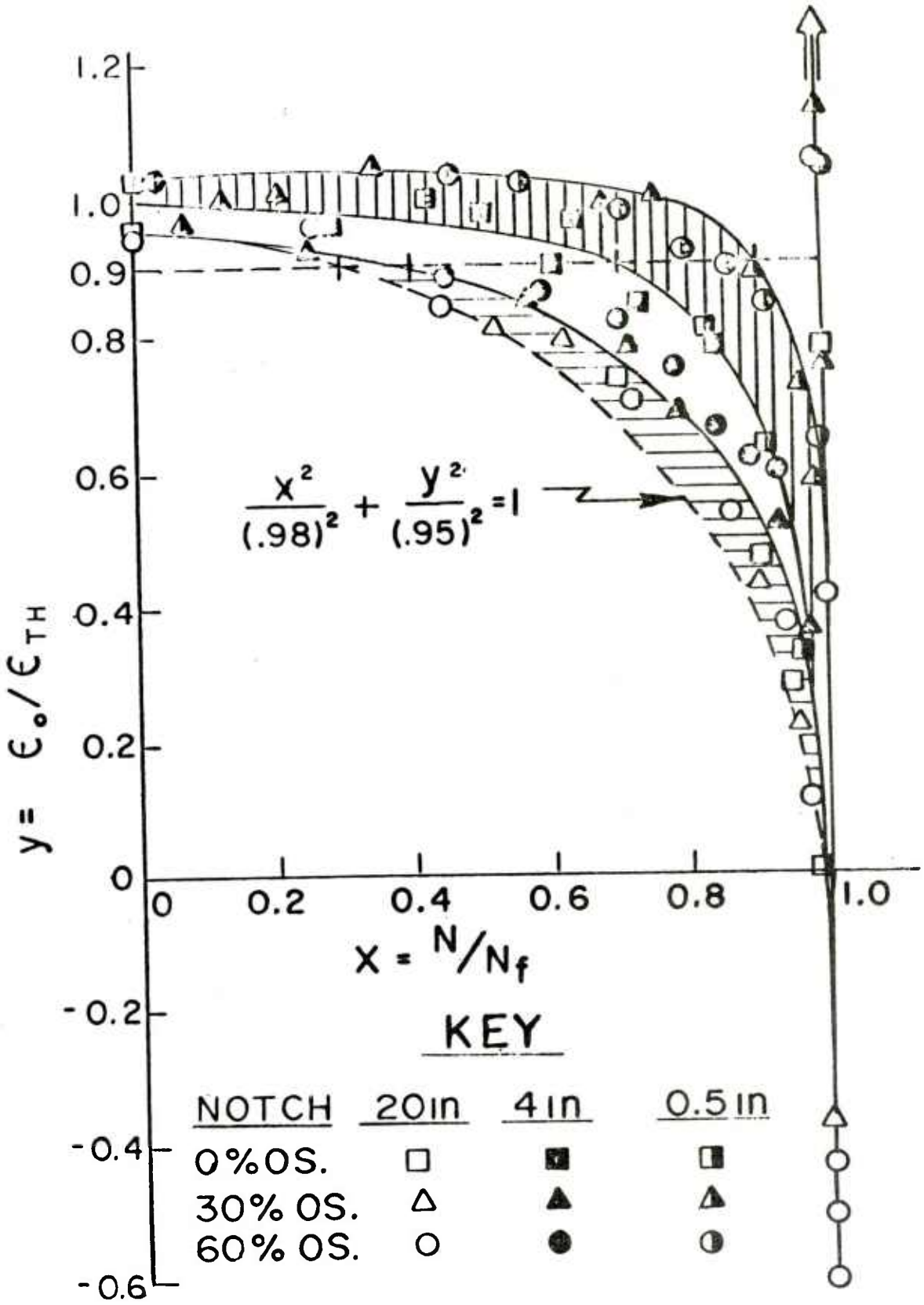

Fig. 10 STRAIN RATIO, ϵ_o/ϵ_{th}, VERSUS FRACTION OF FATIGUE LIFE, N/N_f.

It should be noted that a longer notch of smaller aspect ratio would have required a greater amount of autofrettage in order to endure 10,000 cycles for that depth, and its N/N_f would be smaller than that in the example. Conversely, a semicircular notch would have reached that depth at that number of cycles with less autofrettage and its N/N_f, in the upper band of Figure 10, would be greater.

CONCLUSIONS

(a) The fraction of fatigue life, N/N_f, that has been expended at any given crack depth is indicated by the strain ratio $\varepsilon_o/\varepsilon_{th}$ for particular crack shapes. When ε_o diminishes to zero, failure is imminent. When ε_o has reduced to 90% of the theoretical Lame´ strain, a long curved crack has reached 30 to 40% of life, a semi-elliptical crack has reached 40 to 70% and a semicircular crack has reached 70 to 90% of the fatigue life.

(b) Measurement of the external circumferential strain over the dominant internal crack, along with the determination of the crack depth and shape by ultrasonic technique, enables one to estimate the fraction of fatigue life that has been expended in getting to that crack size.

(c) This procedure provides a practical means of estimating the fatigue life from fatigue tests of only a few cylinders.

REFERENCES

1. Underwood, J. H., Lasselle, R. R., Scanlon, R. D., and Hussain, M. A., "A Compliance K-Calibration for a Pressurized Thick-Walled Cylinder With a Radial Crack," Eng. Fract. Mech., 4, 231-44, (1972).
2. Shannon, R. W. E., "Crack Growth Monitoring by Strain Sensing," Pres. Ves. & Piping, (1), pp. 61-73, Appl. Science Publ. Ltd., England (1973).
3. Throop, J. F. and Fujczak, R. R., "Stress, Strain and Deflection of Cracked C-Shaped Specimens," Experimental Mechanics, Vol. 17, No. 8, pp. 290-296, (1977).
4. Throop, J. F., "Fatigue Crack Growth in Thick-Walled Cylinders," Proceedings National Conference on Fluid Power, Vol. XXVI, pp. 115-131, NCFP, Chicago, (1972).
5. Davidson, T. E., Throop, J. F., and Reiner, A. N., "The Role of Fracture Toughness and Residual Stresses in the Fatigue and Fracture Behavior of Large Thick-Walled Pressure Vessels," Proceedings National Conference on Fluid Power, Vol. XXVI, pp. 102-114, NCFP, Chicago, (1972).
6. Timoshenko, S. P. and Goodier, J. N., Theory of Elasticity, Third Edition, McGraw-Hill Book Company, New York, pp. 68-71 (1970).

TECHNICAL REPORT INTERNAL DISTRIBUTION LIST

	NO. OF COPIES
COMMANDER	1
CHIEF, DEVELOPMENT ENGINEERING BRANCH	1
ATTN: DRDAR-LCB-DA	1
-DM	1
-DP	1
-DR	1
-DS	1
-DC	1
CHIEF, ENGINEERING SUPPORT BRANCH	1
ATTN: DRDAR-LCB-SE	1
-SA	1
CHIEF, RESEARCH BRANCH	2
ATTN: DRDAR-LCB-RA	1
-RC	1
-RM	1
-RP	1
CHIEF, LWC MORTAR SYS. OFC. ATTN: DRDAR-LCB-M	1
CHIEF, IMP. 81MM MORTAR OFC. ATTN: DRDAR-LCB-I	1
TECHNICAL LIBRARY ATTN: DRDAR-LCB-TL	5
TECHNICAL PUBLICATIONS & EDITING UNIT ATTN: DRDAR-LCB-TL	2
DIRECTOR, OPERATIONS DIRECTORATE	1
DIRECTOR, PROCUREMENT DIRECTORATE	1
DIRECTOR, PRODUCT ASSURANCE DIRECTORATE	1

NOTE: PLEASE NOTIFY ASSOC. DIRECTOR, BENET WEAPONS LABORATORY, ATTN: DRDAR-LCB-TL, OF ANY REQUIRED CHANGES.

TECHNICAL REPORT EXTERNAL DISTRIBUTION LIST

	NO. OF COPIES
ASST SEC OF THE ARMY RESEARCH & DEVELOPMENT ATTN: DEP FOR SCI & TECH THE PENTAGON WASHINGTON, D.C. 20315	1
COMMANDER US ARMY MAT DEV & READ. COMD ATTN: DRCDE 5001 EISENHOWER AVE ALEXANDRIA, VA 22333	1
COMMANDER US ARMY ARRADCOM ATTN: DRDAR-LC	1
-LCA (PLASTICS TECH EVAL CEN)	1
-LCE	1
-LCM	1
-LCS	1
-LCW	1
-TSS(STINFO) DOVER, NJ 07801	2
COMMANDER US ARMY ARRCOM ATTN: DRSAR-LEP-L ROCK ISLAND ARSENAL ROCK ISLAND, IL 61299	1
DIRECTOR US Army Ballistic Research Laboratory ATTN: DRDAR-TSB-S (STINFO) ABERDEEN PROVING GROUND, MD 21005	1
COMMANDER US ARMY ELECTRONICS COMD ATTN: TECH LIB FT MONMOUTH, NJ 07703	1
COMMANDER US ARMY MOBILITY EQUIP R&D COMD ATTN: TECH LIB FT BELVOIR, VA 22060	1
COMMANDER US ARMY TANK-AUTMV R&D COMD ATTN: TECH LIB - DRDTA-UL	1
MAT LAB - DRDTA-RK WARREN MICHIGAN 48090	1
COMMANDER US MILITARY ACADEMY ATTN: CHMN, MECH ENGR DEPT WEST POINT, NY 10996	1
COMMANDER REDSTONE ARSENAL ATTN: DRSMI-RB	2
-RRS	1
-RSM ALABAMA 35809	1
COMMANDER ROCK ISLAND ARSENAL ATTN: SARRI-ENM (MAT SCI DIV) ROCK ISLAND, IL 61202	1
COMMANDER HQ, US ARMY AVN SCH ATTN: OFC OF THE LIBRARIAN FT RUCKER, ALABAMA 36362	1
COMMANDER US ARMY FGN SCIENCE & TECH CEN ATTN: DRXST-SD 220 7TH STREET, N.E. CHARLOTTESVILLE, VA 22901	1
COMMANDER US ARMY MATERIALS & MECHANICS RESEARCH CENTER ATTN: TECH LIB - DRXMR-PL WATERTOWN, MASS 02172	2

NOTE: PLEASE NOTIFY COMMANDER, ARRADCOM, ATTN: BENET WEAPONS LABORATORY, DRDAR-LCB-TL, WATERVLIET ARSENAL, WATERVLIET, N.Y. 12189, OF ANY REQUIRED CHANGES.

TECHNICAL REPORT EXTERNAL DISTRIBUTION LIST (CONT)

	NO. OF COPIES
COMMANDER US ARMY RESEARCH OFFICE P.O. BOX 12211 RESEARCH TRIANGLE PARK, NC 27709	1
COMMANDER US ARMY HARRY DIAMOND LAB ATTN: TECH LIB 2800 POWDER MILL ROAD ADELPHIA, MD 20783	1
DIRECTOR US ARMY INDUSTRIAL BASE ENG ACT ATTN: DRXPE-MT ROCK ISLAND, IL 61201	1
CHIEF, MATERIALS BRANCH US ARMY R&S GROUP, EUR BOX 65, FPO N.Y. 09510	1
COMMANDER NAVAL SURFACE WEAPONS CEN ATTN: CHIEF, MAT SCIENCE DIV DAHLGREN, VA 22448	1
DIRECTOR US NAVAL RESEARCH LAB ATTN: DIR, MECH DIV CODE 26-27 (DOC LIB) WASHINGTON, D. C. 20375	1 1
NASA SCIENTIFIC & TECH INFO FAC P. O. BOX 8757, ATTN: ACQ BR BALTIMORE/WASHINGTON INTL AIRPORT MARYLAND 21240	1
COMMANDER DEFENSE TECHNICAL INFO CENTER ATTN: DTIA-TCA CAMERON STATION ALEXANDRIA, VA 22314	12
METALS & CERAMICS INFO CEN BATTELLE COLUMBUS LAB 505 KING AVE COLUMBUS, OHIO 43201	1
MECHANICAL PROPERTIES DATA CTR BATTELLE COLUMBUS LAB 505 KING AVE COLUMBUS, OHIO 43201	1
MATERIEL SYSTEMS ANALYSIS ACTV ATTN: DRXSY-MP ABERDEEN PROVING GROUND MARYLAND 21005	1

NOTE: PLEASE NOTIFY COMMANDER, ARRADCOM, ATTN: BENET WEAPONS LABORATORY, DRDAR-LCB-TL, WATERVLIET ARSENAL, WATERVLIET, N.Y. 12189, OF ANY REQUIRED CHANGES.